Inorganica Chimica Acta 387 (2012) 145–150

Contents lists available at SciVerse ScienceDirect

Inorganica Chimica Acta

journal homepage: www.elsevier.com/locate/ica

# First examples of luminescent zinc(II)-bisquinoxalinato complexes: Synthesis, spectroscopic and theoretical studies

Andrew J. Hallett *, Simon J.A. Pope

*School of Chemistry, Cardiff University, Main Building, Park Place, Cardiff CF10 3AT, UK*

ARTICLE INFO

*Article history:*
Received 19 October 2011
Accepted 4 January 2012
Available online 11 January 2012

*Keywords:*
5-Hydroxyquinoxaline
Zn(II) complexes
Photophysical properties
DFT studies
OLEDs

ABSTRACT

Four novel homoleptic zinc(II) complexes were prepared in high yield from *para*-substituted 2,3-diphenyl-5-hydroxyquinoxaline ligands, **LH$^n$**, giving **[Zn(L$^n$)$_2$]**. Density functional theoretical calculations were performed to probe the influence of the variation in *para*-substitution on the ligands. The calculations suggest that ligand-centred character appears to dominate the HOMO and LUMOs. Experimental electrochemical and spectroscopic characterisation showed that the subtle variations in absorption and emission wavelengths are due to ligand-dominated transitions that are influenced by electronic nature of the *para*-substituted phenyl units in coordinated **L$^n$**, in both solution and the solid states.

## 1. Introduction

In recent years there has been an increasing interest in metal complexes with luminescent properties for use in a multitude of areas, in particular photovoltaics, OLEDs, responsive probes and biological imaging [1]. These complexes contain chromophores, which can be modified in order to tune the wavelength of emitted light. 8-Hydroxyquinoline metal complexes are some of the most reliable electro-transporting and emitting materials used in OLEDs due to their thermal stability, high fluorescence and electron transporting mobility [2]. Whilst there have been numerous reports on metal ion complexes of Al(III) containing commercially available 8-hydroxyquinoline derivatives [1f,3], by comparison, relatively few describe the incorporation of substituted hydroxyquinoline ligands into zinc(II) complexes. OLEDs based upon the benchmark tris(8-hydroxyquinolinato)aluminium, $Alq_3$, (Fig. 1) complex possess an electroluminescence efficiency (quantum yield) which is limited to a maximum of 25% [4]. However, the zinc(II) analogue, $Znq_2$, (Fig. 1) has better injection efficiency, lower operating voltage, and higher quantum yield [5]. Therefore, zinc complexes of this type have a great potential in electroluminescent (EL) devices. Recently, it has been reported that the emission wavelength of these complexes can be easily tuned by modifying the 8-hydroxyquinoline ligands in the 2-, 5- and 7-positions [6]. Here we report the first examples of zinc(II) complexes bearing substituted hydroxyquinoxaline ligands in which the 2- and 3-positions contain *para*-substituted phenyl groups. The synthesis, characterisation and spectroscopic properties are reported herein.

## 2. Experimental

### 2.1. Materials and Instruments

All reactions were performed with the use of vacuum line and Schlenk techniques. Reagents were commercial grade and were used without further purification. $^1$H NMR spectra and were run on an NMR-FT Bruker 400 MHz spectrometer and were recorded in d$^6$-DMSO. $^1$H NMR chemical shifts ($\delta$) were determined relative to internal TMS and are given in ppm. Mass spectra were carried out by the staff at Cardiff University. High resolution mass spectra were carried out by at the EPSRC National Mass Spectrometry Service at Swansea University. UV–Vis studies were performed on a Jasco V-570 spectrophotometer as DMF solutions ($5 \times 10^{-5}$ M). Photophysical data were obtained on a JobinYvon–Horiba Fluorolog spectrometer fitted with a JY TBX picosecond photodetection module as MeOH solutions or in the solid state. Emission spectra were uncorrected and excitation spectra were instrument corrected. The pulsed source was a Nano-LED configured for 372 nm output operating at 500 or 100 kHz. Luminescence lifetime profiles were obtained using the JobinYvon–Horiba FluoroHub single photon counting module and the data fits yielded the lifetime values using the provided DAS6 deconvolution software. The ligands **LH$^n$** ($n$ = 1–4) were prepared as previously reported [7].

---

* Corresponding author. Tel.: +44 029 20879316; fax: +44 029 20874030.
*E-mail address:* hallettaj@cardiff.ac.uk (A.J. Hallett).

0020-1693/$ - see front matter © 2012 Elsevier B.V. All rights reserved.
doi:10.1016/j.ica.2012.01.008

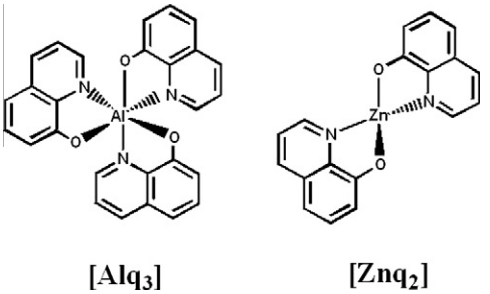

**Fig. 1.** The structures of $Alq_3$ and $Znq_2$.

### 2.2. Electrochemistry

Electrochemical studies were carried out using a Parstat 2273 potentiostat in conjunction with a three-electrode cell. The auxiliary electrode was a platinum wire and the working electrode a platinum (1.0 mm diameter) disc. The reference was a silver wire separated from the test solution by a fine-porosity frit. Solutions (10 ml DMF) were $1 \times 10^{-3}$ mol $dm^{-3}$ in the test compound and 0.1 mol $dm^{-3}$ in $[NBu_4][PF_6]$ as the supporting electrolyte. Solutions were de-oxygenated with a stream of $N_2$ gas and were maintained under a positive pressure of $N_2$ during all measurements. Potentials are quoted versus the $[Fe(\eta^5\text{-}C_5H_5)_2]^+/[Fe(\eta^5\text{-}C_5H_5)_2]$ couple ($E^{0\prime}$ = + 0.45 V in DMF) [8] as the internal standard.

### 2.3. DFT studies

All calculations were performed on the Gaussian 03 program [9]. Geometry optimisations were carried out without constraints using the B3PW91 functional. The LANL2DZ basis set was used for the Zn centres, and was invoked with pseudo-potentials for the core electrons, a 6–31G(d,p) basis set for all coordinating atoms with a 6–31G basis set for all remaining atoms. All optimisations were followed by frequency calculations to ascertain the nature of the stationary point (minimum or saddle point).

### 2.4. Synthesis

#### 2.4.1. ***$[Zn(L^1)_2]$***

$Zn(OAc)_2{\cdot}2H_2O$ (25 mg, 0.11 mmol), **$LH^1$** (69 mg, 0.23 mmol), $Na_2CO_3$ (122 mg, 1.15 mmol) and 2-methoxyethanol (8 ml) were heated at 110 °C for 14 h. The mixture was cooled to room temp and the product precipitated by the slow addition of water (25 ml). The orange powder was filtered, washed with water and dried *in vacuo*. Yield 66 mg, 0.10 mmol (88%). $^1H$ NMR (400 MHz, $d^6$-DMSO) $\delta_H$ = 7.71 (2H, app. t {coincident dd}, $^3J_{HH}$ = 8.1 Hz), 7.36–7.28 (14H, m), 7.15 (2H, d, $^3J_{HH}$ = 8.3 Hz), 6.99 (2H, d, $^3J_{HH}$ = 7.5 Hz), 6.87 (6H, m) ppm. EI MS found *m/z* 660.1, calculated *m/z* 660.1 for $[M]^+$. HR MS found *m/z* 658.1344, calculated *m/z* 658.1342 for $[C_{40}H_{26}O_2N_4Zn_1]^+$. UV–Vis (DMF): $\lambda_{max}$ ($\varepsilon$ $dm^3\ mol^{-1}\ cm^{-1}$) = 302(44 500), 320(38 150), 465(2400) nm.

#### 2.4.2. ***$[Zn(L^2)_2]$***

Prepared similarly from $Zn(OAc)_2{\cdot}2H_2O$ (16 mg, 0.07 mmol) and **$LH^2$** (69 mg, 0.15 mmol). Yield 64 mg, 0.67 mmol (91%). $^1H$ NMR (400 MHz, $d^6$-DMSO) $\delta_H$ = 7.72 (2H, app. t, $^3J_{HH}$ = 8.2 Hz), 7.63 (2H, d, $^3J_{HH}$ = 8.3 Hz), 7.51 (4H, d, $^3J_{HH}$ = 8.4 Hz), 7.19 (4H, d, $^3J_{HH}$ = 8.5 Hz), 7.13 (2H, d, $^3J_{HH}$ = 8.4 Hz), 7.09–6.92 (8H, m) ppm. Negative ion MS found *m/z* 1010.7, calculated *m/z* 1011.1 for $[M+Cl]^-$. HR MS found *m/z* 1004.7473, calculated *m/z* 1004.7462 for $[C_{40}H_{22}O_2N_4Br_4Cl_1Zn_1]^-$. UV–Vis (DMF): $\lambda_{max}$ ($\varepsilon$ $dm^3\ mol^{-1}\ cm^{-1}$) = 300(54 500), 320(57 300), 363(16 350), 459(2650) nm.

#### 2.4.3. ***$[Zn(L^3)_2]$***

Prepared similarly from $Zn(OAc)_2{\cdot}2H_2O$ (32 mg, 0.14 mmol) and **$LH^3$** (95 mg, 0.29 mmol). Yield 86 mg, 0.24 mmol (82%). $^1H$ NMR (400 MHz, $d^6$-DMSO) $\delta_H$ = 7.66 (2H, app. t, $^3J_{HH}$ = 8.3 Hz), 7.22 (2H, d, $^3J_{HH}$ = 8.4 Hz), 7.11 (6H, app. t, $^3J_{HH}$ = 8.2 Hz), 6.97 (4H, d, $^3J_{HH}$ = 7.9 Hz), 6.91 (4H, br s), 6.45 (4H, d, $^3J_{HH}$ = 7.8 Hz) ppm. ES MS found *m/z* 717.2, calculated *m/z* 717.2 for $[M+H]^+$. HR MS found *m/z* 715.2055, calculated *m/z* 715.2046 for $[C_{44}H_{35}O_2N_4Zn_1]^+$. UV–Vis (DMF): $\lambda_{max}$ ($\varepsilon$ $dm^3\ mol^{-1}\ cm^{-1}$) = 294(16 600), 353(3500), 475(400) nm.

#### 2.4.4. ***$[Zn(L^4)_2]$***

Prepared similarly from $Zn(OAc)_2{\cdot}2H_2O$ (17 mg, 0.08 mmol) and **$LH^4$** (57 mg, 0.16 mmol). Yield 53 mg, 0.07 mmol (88%). $^1H$ NMR (400 MHz, $d^6$-DMSO) $\delta_H$ = 7.63 (2H, app. t, $^3J_{HH}$ = 8.5 Hz), 7.14 (4H, d, $^3J_{HH}$ = 8.6 Hz), 7.06 (2H, d, $^3J_{HH}$ = 8.1 Hz), 6.94 (6H, m), 6.82 (4H, d, $^3J_{HH}$ = 8.6 Hz), 6.25 (4H, d, $^3J_{HH}$ = 8.5 Hz), 3.74 (6H, s), 3.46 (6H, s) ppm. ES MS found *m/z* 803.2, 819.2 and 844.1, calculated *m/z* 803.2, 819.3 and 844.2 for $[M+Na]^+$, $[M+K]^+$ and $[M+MeCN+Na]^+$ respectively. HR MS found *m/z* 801.1656, calculated *m/z* 801.1662 for $[C_{44}H_{34}O_6N_4Na_1Zn_1]^+$. UV–Vis (DMF): $\lambda_{max}$ ($\varepsilon$ $dm^3\ mol^{-1}\ cm^{-1}$) = 301(11 800), 329(8400), 377(5000), 479(550) nm.

## 3. Results and discussion

### 3.1. Synthesis and characterisation

Four *para*-substituted 2,3-diphenyl-5-hydroxyquinoxaline ligands, **$LH^{1-4}$** (1 = *p*-H, 2 = *p*-Br, 3 = *p*-Me, 4 = *p*-OMe) were prepared in a two-step reaction (Scheme 1) as previously reported [7]. Firstly, 2-amino-3-nitrophenol was reduced by heating to reflux in acidic EtOH for 14 h in the presence of zinc dust, giving the corresponding 2,3-diamino compound. Subsequent condensation with a range of substituted diones in refluxing EtOH for 16 h gave the desired ligands as yellow powders.

The neutrally charged homoleptic complexes **$[Zn(L^n)_2]$** (*n* = 1–4) were isolated, following addition of base to a reaction mixture composition of 2:1 ligand to $Zn(OAc)_2{\cdot}2H_2O$ in 2-methoxyethanol, in excellent yields of 82–91%. The complexes were isolated by addition of water to the reaction mixture as bright orange/red powders. They were characterised in the solution state using $^1H$ NMR, UV–Vis. and luminescence spectroscopy and cyclic voltammetry. EI mass spectrometry revealed the parent ions $[M]^+$ for **$[Zn(L^1)_2]$**, negative ion revealed $[M+Cl]^-$ for **$[Zn(L^2)_2]$** and ES mass spectrometry revealed the protonated parent ions $[M+H]^+$ for **$[Zn(L^3)_2]$** and **$[Zn(L^4)_2]$**.

### 3.2. Density functional theory (DFT) studies

In order to understand the nature of the electronic transitions within this class of complex, DFT calculations (computed using the B3PW91 hybrid orbital) were undertaken. In these examples, an assessment of the frontier orbitals provided a qualitative insight into the HOMO (highest occupied molecular orbital) and LUMO (lowest unoccupied molecular orbital) energy levels.

Firstly, for the quinoxalinato complexes described here the lowest energy configurations show that the predicted structures have one of the two phenyl rings twisted out of the plane for both ligands in each case. The calculated energy levels of both the HOMO and HOMO-1 are sufficiently similar ($\Delta E$ < 0.2 eV) to be considered isoenergetic in all cases. The same is true of the LUMO and LUMO+1. Both the HOMO and LUMO are located primarily on the quinoxalinato ligand with little or no orbital coverage on the metal centre. The HOMO lies exclusively on one of the quinoxalinato ligands with the HOMO-1 (a mirror image) on the second

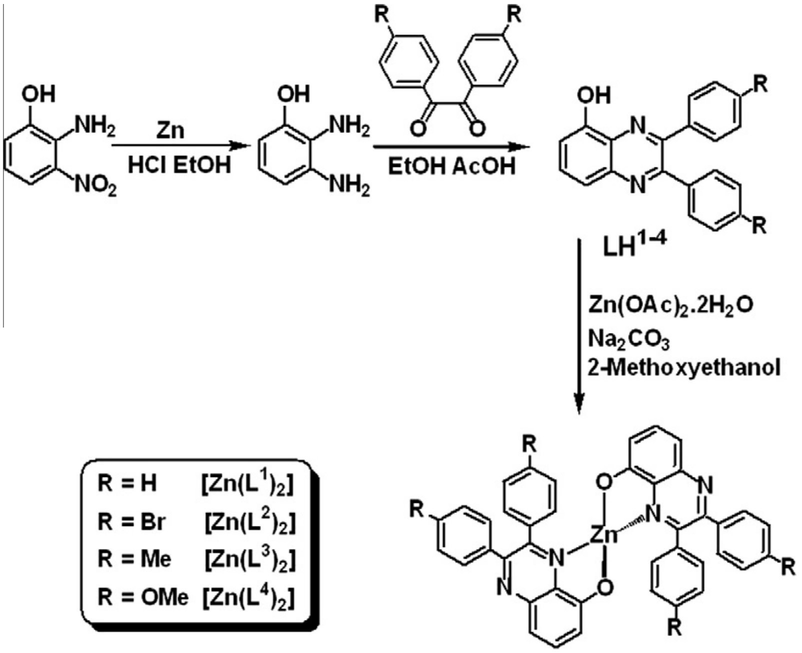

**Scheme 1.** Synthetic route to ligands **LH$^n$** and complexes [**Zn(L$^n$)$_2$**] ($n$ = 1–4).

quinoxalinato ligand. As these are isoenergetic, they have been depicted together (Fig. 2). Again, LUMO and LUMO+1 are mirror images and are depicted as one.

The HOMO orbitals are more delocalised over the phenolato moieties while the LUMOs are over the pyrazine moieties, although this effect is not as exaggerated as for quinoline complexes [10]. There is no direct contribution from the substituted phenyl rings to the HOMO coverage, however, the nature of the *para*-substituent does appear to impart an influence on the overall energy level. For example, the complex of the electron withdrawing *para*-Br ligand **[Zn(L$^2$)$_2$]** has the lowest HOMO energy level ($E$ = −5.66 eV) whereas the complex of the electron donating *para*-OMe **[Zn(L$^4$)$_2$]** has the highest ($E$ = −5.12 eV). Similarly, the LUMO energies also reflect this variation (*para*-Br $E_{\mathrm{LUMO}}$ = −2.67 eV; *para*-OMe $E_{\mathrm{LUMO}}$ = −2.07 eV). This calculated data suggests that variation of the remote *para* substituent can lead to a degree of tunable optical

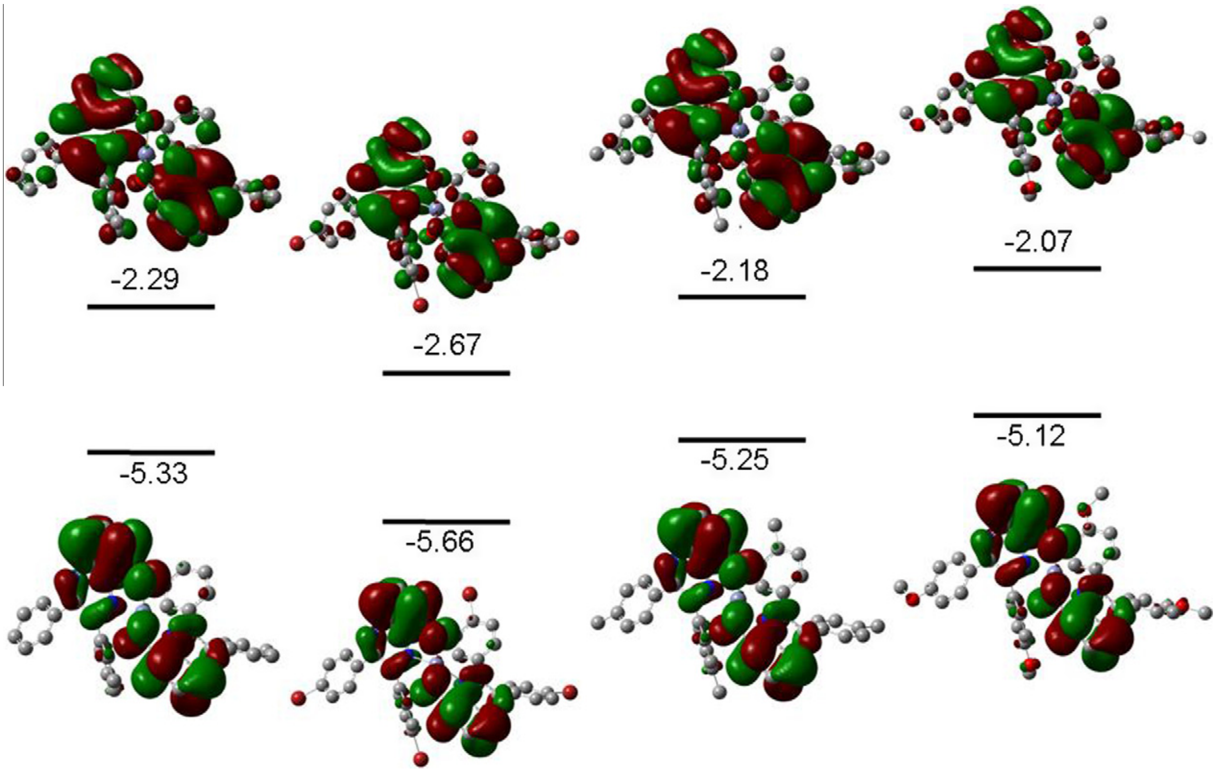

**Fig. 2.** Graphical representation of the frontier orbitals of **[Zn(L$^n$)$_2$]** ($n$ = 1–4 left to right). Bottom, HOMOs; top, LUMOs (energy levels are in eV).

properties within this series of complexes. Interestingly, the calculated HOMO–LUMO bandgaps do not vary a great deal (2.99–3.07 eV).

### 3.3. Cyclic voltammetry

An investigation into the electrochemical behaviour of the four complexes was undertaken in deaerated DMF. Electrochemical studies were performed in order to approximate the HOMO energy levels for each complex. The cyclic voltammograms, measured at a platinum disc electrode (scan rate 200 mV $s^{-1}$, $1 \times 10^{-3}$ M solutions, 0.1 M $[NBu_4][PF_6]$ as a supporting electrolyte) of the complexes **$[Zn(L^n)_2]$** ($n = 1–4$) each showed one oxidation, which were not fully reversible (Table 1). One or two irreversible reductions were also observed which can be assigned to the reduction of the quinoxaline moiety [11].

The oxidation potential varies very little across the series of complexes (0.95–1.00 V): the difference in oxidation potentials is presumably due to the subtle donor variations of the substituted quinoxalinato ligands. The $E_{HOMO}$ values were calculated using the reported equations [12] and the resultant values, ranging from −5.28 to −5.33 eV, are detailed in Table 1.

### 3.4. Photophysical properties

The UV–Vis absorption spectra of the complexes were measured as aerated DMF solutions. The complexes all absorb in the visible region (Fig. 3, Table 1): the features are in the range 300–550 nm and are typically broad in appearance. The absorption properties are dominated by a broad visible absorption around 320–400 nm attributed to IL $\pi$–$\pi^*$ transitions, possibly including phenoxide-to-pyrazine charge transfer. The electronic nature of the *para*-substituted groups subtly influences the positioning of this absorption band. Indeed, complexes of the relatively electron poor Ph and *para*-Br substituted ligands, **$[Zn(L^1)_2]$** and **$[Zn(L^2)_2]$** respectively, possess similar absorption maxima (~320 nm), whereas the complex of the electron-donating *para*-OMe substituted ligand, **$[Zn(L^4)_2]$**, showed a significant bathochromic shift (377 nm). The complexes each exhibit a relatively weak absorption band that tails into the visible region. Since Zn(II) to quinoxaline ring charge transfer (MLCT) is ruled out, the relatively weak absorption bands from 400 to 550 nm are assigned to intra-ligand charge transfer ($^1$ILCT) transitions [13].

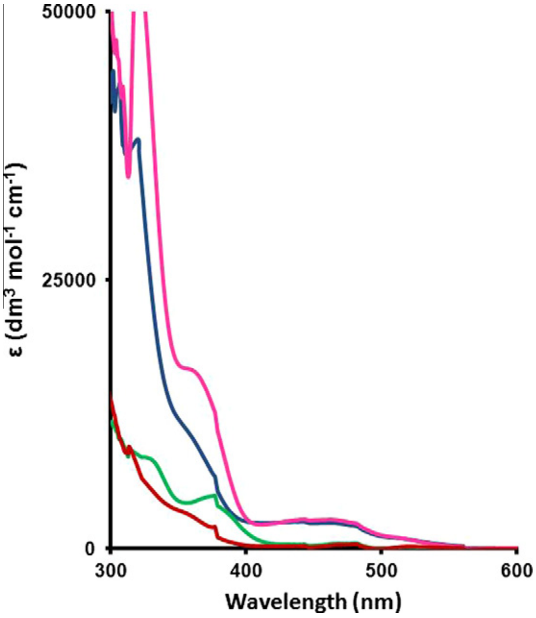

**Fig. 3.** UV–Vis spectrum of **$[Zn(L^1)_2]$** (blue), **$[Zn(L^2)_2]$** (purple), **$[Zn(L^3)_2]$** (red) and **$[Zn(L^4)_2]$** (green) recorded as $5 \times 10^{-5}$ M DMF solutions. (For interpretation of the references to colour in this figure legend, the reader is referred to the web version of this article.)

Luminescence measurements were conducted on MeOH solutions of the complexes (Table 1, Fig. 4). It has been reported that the luminescent behaviour of zinc(II) hydroxyquinolinato complexes can be varied by modification at the 2-position of the 8-hydroxyquinoline rings [14]. Here we have functionalised the quinoxaline group in the 2- and 3-positions. The emission maxima are in the range 451–480 nm showing a degree of tunability within the series of complexes as well as slight differences from the free ligands, which are emissive in the region 438–474 nm [7]. The complexes **$[Zn(L^1)_2]$** and **$[Zn(L^2)_2]$** show slightly blue shifted emission compared to the ligands whereas **$[Zn(L^3)_2]$** and **$[Zn(L^4)_2]$** are red shifted. As it is not possible for $d^{10}$ zinc complexes to undergo low energy charge transfer or participate in metal-centred transitions, the excited states of these Zn(II) complexes are classically ligand-centred (LC) in nature [15]. Therefore, the emission from **$[Zn(L^n)_2]$** is believed to arise from an excited state centred on the quinoxalinato ligand in each case. Related quinolinato complexes of Al(III) have shown that there is also significant CT character that originates from intra-ligand phenoxide-to-pyridine transitions [16]. Our DFT studies suggest that a similar electronic character is inherent within the Zn complexes described here. The calcula-

**Table 1**
Absorption, emission and electrochemical properties of the zinc(II) complexes.

| Complex | $\lambda_{max}$ ($\varepsilon$/M$^{-1}$ cm$^{-1}$) (nm)[a] | $E_{ox}$ (V)[b] | HOMO (eV)[c] | $E_{bandgap}$ (eV)[d] | LUMO (eV)[e] | $\lambda_{em}$ (nm) | $\tau$ (ns) aerated[f] | $\lambda_{em}$ (solid) (nm) | $\tau$ (ns) solid[f] |
|---|---|---|---|---|---|---|---|---|---|
| **$[Zn(L^1)_2]$** | 302(44500), 320(38150),465(2400) | 0.98 | −5.31 | 2.05 | −3.26 | 451 | <1 (70%), 2.6 (30%) | 623 | <1 |
| **$[Zn(L^2)_2]$** | 300(54500), 320(57300), 363(16350), 459(2650) | 1.00 | −5.33 | 2.09 | −3.24 | 458, 480 | <1 (62%), 2.1 (38%),<1 (52%)[g], 2.8 (48%)[g] | 618 | <1 |
| **$[Zn(L^3)_2]$** | 294(16600), 353(3500),475(400) | 0.96 | −5.29 | 2.07 | −3.22 | 476 | <1 (62%), 1.9 (38%) | 613 | <1 |
| **$[Zn(L^4)_2]$** | 301(11800), 329(8400), 377(5000), 479(550) | 0.95 | −5.28 | 2.11 | −3.17 | 456 | <1 (31%), 1.9 (69%) | 606 | <1 |

[a] Absorption spectra measured as DMF solutions ($5 \times 10^{-5}$ mol dm$^{-3}$).

[b] Oxidation potentials measured as DMF solutions at 200 mV $s^{-1}$ with 0.1 M $[NBu_4][PF_6]$ as supporting electrolyte calibrated with $FeCp_2/FeCp_2^+$.

[c] The HOMO energy level was calculated using the equation $-HOMO\ (eV) = E_{ox} - E_{Fc/Fc^+} + 4.8$.

[d] $E_{bandgap}$ was determined from the absorption edge of the zinc complexes.

[e] The LUMO energy level was calculated using the equation LUMO (eV) = HOMO + $E_{bandgap}$.

[f] Excitation at 372 nm.

[g] Emission at 480 nm.

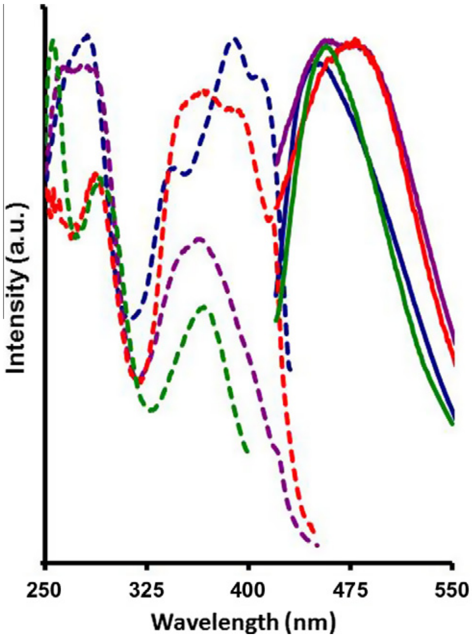

**Fig. 4.** Excitation (dashed) and emission (solid) spectra of **[Zn(L$^1$)$_2$]** (blue), **[Zn(L$^2$)$_2$]** (red), **[Zn(L$^3$)$_2$]** (pink) and **[Zn(L$^4$)$_2$]** (green) recorded as MeOH solutions. (For interpretation of the references to colour in this figure legend, the reader is referred to the web version of this article.)

tions propose that the HOMO in each case comprises significant phenolate character; in each case the LUMO has significant pyrazine-localised electron density.

The complex **[Zn(L$^2$)$_2$]** (*p*-Br) shows emission bands at 458 and 480 nm. This dual emissive behaviour has been previously reported for 2-(2-hydroxyphenyl)benzoxazolate zinc complexes and is due to the $\pi$–$\pi^*$ transition as well as short-lived excimer formation in the excited state [17].

In order to fully examine the emissive nature of the complexes, luminescence spectra were also measured in the solid state (Table 1, Fig. 5). Each of the complexes absorbs from 350 to 550 nm and are emissive in the region 606–623 nm (with no emission in the range 450–480 nm), again noting a degree of tunability with variation of the *para*-substituents on the phenyl rings. Luminescence lifetimes are short ($\tau$ = < 5 ns) in both the solid and solution states.

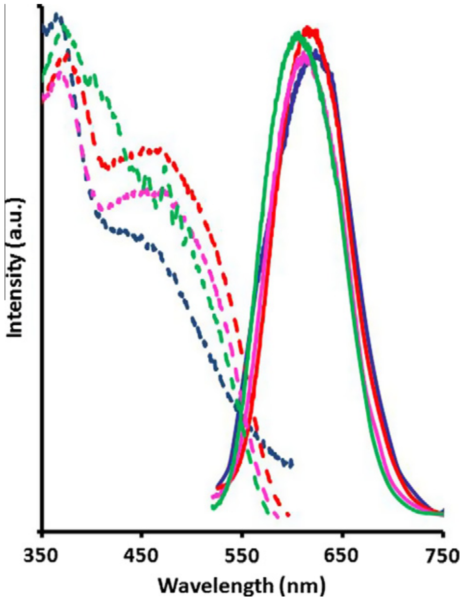

**Fig. 5.** Excitation (dashed) and emission (solid) spectra of **[Zn(L$^1$)$_2$]** (blue), **[Zn(L$^2$)$_2$]** (red), **[Zn(L$^3$)$_2$]** (pink) and **[Zn(L$^4$)$_2$]** (green) recorded as solids. (For interpretation of the references to colour in this figure legend, the reader is referred to the web version of this article.)

## 4. Conclusions

This paper describes the first examples of homoleptic Zn(II) complexes containing functionalised quinoxalinato-based ligands. Variation of the *para*-phenyl substituents in the 2- and 3-positions of the quinoxaline ring provides the means for moderately tuning the electronic characteristics of the complexes. Complexes are generally emissive in the 450–480 nm region in solution and 600–620 nm in the solid state. Experimentally, a clear trend is evident in the complexes in the solid state whereby an electron-withdrawing group (**L$^2$**) red-shifts the emission peak, but an electron donating group blue-shifts (**L$^4$**). The wavelength variations within this series demonstrate an ability to tune the emission character of the complexes as a function of the remote *para* substituent of the ligands.

Supporting DFT calculations suggest that both the HOMO and LUMOs are completely localised on the coordinated quinoxalinato ligands. Spectroscopically, this facilitates a degree of tuning in the electronic properties of the complexes, whilst the photophysical properties of the complexes appear to be dominated by ligand-centred character.

## Acknowledgements

The EPSRC are thanked for funding. Dr. Robert Jenkins, Mr. Robin Hicks and Mr. David Walker are thanked for running low resolution mass spectra. The staff of the EPSRC MS National Service at the University of Swansea are also gratefully acknowledged.

## References

[1] (a) V.W.W. Yam, K.K.W. Lo, Coord. Chem. Rev. 184 (1998) 157;
(b) M.W. Cooke, G.S. Hanan, Chem. Soc. Rev. 36 (2007) 1466;
(c) J.N. Demas, B.A. DeGraff, Coord. Chem. Rev. 211 (2001) 317;
(d) M. Bartholomii, J. Valliant, K.P. Maresca, J. Babich, J. Zubieta, Chem. Commun. (2009) 493;
(e) L. Fabrizzi, M. Liechelli, A. Taglietti, Dalton Trans. (2003) 3471;
(f) C.W. Tang, S.A. Van Slyke, Appl. Phys. Lett. 51 (1987) 913;
(g) E. Baranoff, J.H. Yum, M. Graetzel, M.K. Nazeeruddin, J. Organomet. Chem. 694 (2009) 2661.
[2] (a) M. Binkmann, B. Fite, S. Pratontep, C. Chaumont, Chem. Mater. 16 (2004) 4627;
(b) M.B. Khalifa, D. Vaufrey, J. Tardy, Org. Electron. 5 (2004) 187;
(c) M. Miraee, M.M. Amini, Appl. Organomet. Chem. 19 (2005) 339.
[3] K. Müllen, U. Scherf (Eds.), Organic Light-Emitting Diodes, Wiley-VCH, Weinheim, 2006.
[4] C.W. Tang, Coord. Chem. Rev. 215 (2001) 79.
[5] A. Meyers, C. South, M. Week, Chem. Commun. (2004) 1176;
(b) L.S. Sapochak, F.E. Benincasa, R.S. Schofield, J.L. Baker, K.K.C. Riccio, D. Fogarty, H. Kohlmann, K.F. Ferris, P.E. Burrows, J. Am. Chem. Soc. 124 (2002) 6119;
(c) T.A. Hopkins, K. Meerholz, S. Shaheen, M.L. Anderson, A. Schmidt, B. Kippelen, A.B. Padias, J.H.K. Hall, N. Peyghambarian, N.R. Armstrong, Chem. Mater. 8 (1996) 344;
M. Ghedini, M. La Deda, I. Aiello, A. Grisolia, Synth. Met. 138 (2003) 189.
[6] (a) M. Gredini, M.L. Deda, I. Aiello, A. Grisolia, Inorg. Chim. Acta 357 (2004) 33;
(b) R. Pohl, V.A. Motes, J. Shinar, P. Anzenbacher, J. Org. Chem. 69 (2004) 1723;
(c) V.P. Barberis, J.A. Mikroyannidid, Synth. Met. 156 (2006) 865.
[7] A.J. Hallett, B.M. Kariuki, S.J.A. Pope, Dalton Trans. 40 (2011) 9474.
[8] N.G. Connelly, W.E. Geiger, Chem. Rev. 96 (1996) 877.
[9] M.J. Frisch, G.W. Trucks, H.B. Schlegel, G.E. Scuseria, M.A. Robb, J.R. Cheeseman, J.A. Montgomery Jr., T. Vreven, K.N. Kudin, J.C. Burant, J.M. Millam, S.S. Iyengar, J. Tomasi, V. Barone, B. Mennucci, M. Cossi, G. Scalmani, N. Rega, G.A. Petersson, H. Nakatsuji, M. Hada, M. Ehara, K. Toyota, R. Fukuda, J. Hasegawa, M. Ishida, T. Nakajima, Y. Honda, O. Kitao, H. Nakai, M. Klene, X. Li, J.E. Knox, H.P. Hratchian, J.B. Cross, V. Bakken, C. Adamo, J. Jaramillo, R. Gomperts, R.E. Stratmann, O. Yazyev, A.J. Austin, R. Cammi, C. Pomelli, J.W. Ochterski, P.Y. Ayala, K.

Morokuma, G.A. Voth, P. Salvador, J.J. Dannenberg, V.G. Zakrzewski, S. Dapprich, A.D. Daniels, M.C. Strain, O. Farkas, D.K. Malick, A.D. Rabuck, K. Raghavachari, J.B. Foresman, J.V. Ortiz, Q. Cui, A.G. Baboul, S. Clifford, J. Cioslowski, B.B. Stefanov, G. Liu, A. Liashenko, P. Piskorz, I. Komaromi, R.L. Martin, D.J. Fox, T. Keith, M.A. Al-Laham, C.Y. Peng, A. Nanayakkara, M. Challacombe, P.M.W. Gill, B. Johnson, W. Chen, M.W. Wong, C. Gonzalez, J.A. Pople, GAUSSIAN 03, Revision E.01. GAUSSIAN, Inc., Wallingford, CT, 2004.

[10] (a) R. Vivas-Reyes, F. Núñez-Zarur, E. Martínez, Org. Electron. 9 (2008) 625;
(b) L. Chen, P. Tao, C. Sun, X. Kiu, B. Xu, Synth. Met. 161 (2011) 1145.

[11] (a) Y. Nakabayashi, Y. Masuda, E. Sekido, J. Electroanal. Chem. 205 (1986) 209;
(b) X. Chen, D. Qiu, L. Ma, Y. Cheng, Y. Geng, Z. Xie, L. Wang, Trans. Met. Chem. 31 (2006) 639.

[12] (a) A. Mishra, P.K. Nayak, D. Ray, M.P. Patankar, K.L. Narasimhan, N. Periasamy, Tetrahedron Lett 47 (2006) 4715;
(b) B.W.D. Andrade, S. Datta, S.R. Forrest, P. Djurovich, E. Polikarpov, M.E. Thompson, Org. Electron. 6 (2005) 11.

[13] X-Y. Wang, A.D. Guerzo, R.H. Schmehl, Chem. Commun. (2002) 2344.

[14] A. Sharma, D. Singh, J.K. Makrandi, M.N. Kamalasanan, R. Shrivastva, I. Singh, Mater. Lett. 61 (2007) 4614.

[15] (a) I. García-Santos, J. Sanmartín, A.M. García-Deibe, M. Fondo, E. Gómez, Inorg. Chim. Acta 363 (2010) 193;
(b) C.L. Dolberg, C. Turro, Inorg. Chem. 40 (2001) 2484;
(c) D.M. Roundhill, Photochemistry and Photophysics of Metal Complexes, in: J.P. Fackler (Ed.), Modern Inorganic Chemistry Series, Plenum Press, New York, 1994, pp. 56–57.

[16] V.A. Montes, R. Pohl, J. Shinar, P. Anzenbacher Jr., Chem. Eur. J. 12 (2006) 4523.

[17] V.K. Rai, R. Srivastava, M.N. Kamalasanan, J. Lumin. 130 (2010) 249.